JLAB-PHY-01-23
WM-01-112

The deuteron: a mini-review

Franz Gross[*†] and R. Gilman[**†]

[*]*Department of Physics, College of William and Mary, Williamsburg, VA 23187, USA*
[†]*Jefferson Laboratory, 12000 Jefferson Avenue, Newport News, VA 23606, USA*
[**]*Rutgers University, 136 Frelinghuysen Rd, Piscataway, NJ 08855, USA*

Abstract. We review[1] some recent results for elastic electron deuteron scattering (deuteron form factors) and photodisintegration of the deuteron, with emphasis on the recent high energy data from Jefferson Laboratory (JLab).

DEUTERON WAVE FUNCTIONS AND FORM FACTORS

Calculations of deuteron form factors and photo and electrodisintegration to the NN final state require a deuteron wave function. The best nonrelativistic wave functions are calculated from the Schrödinger equation using a potential adjusted to fit the NN scattering data for lab energies from 0 to 350 MeV. The quality of realistic potentials have improved steadily, and now the best potentials give fits to the NN database with a χ^2/d.o.f $\simeq 1$. The Paris potential [2] was among the first potentials to be determined from such realistic fits, and it has since been replaced by the Argonne V18 potential (denoted by AV18) [3], the Nijmegen potentials [4], and most recently by the CD Bonn potentials [5, 6]. The momentum space S and D state wave functions determined from three of these models and two relativistic models (Model IIB [7] and Model W16, one of a family of models with varying amounts of off-shell sigma coupling introduced in connection with relativistic calculations of the triton binding energy described in Ref. [8]) are shown in Fig. 1. The figure shows that the S and D-state components of all of these models are almost identical (i.e.variations of less than 10%) for momenta below about 400 MeV, and vary by less than a factor of 2 as the momenta reaches 1 GeV.

Elastic electron–deuteron scattering is described in the one-photon exchange approximation by three deuteron form factors [9, 10, 11]. In its most general form, the relativistic deuteron current can be written [9, 12]

$$-\langle d'|J^\mu|d\rangle = \left\{ G_1(Q^2)\,[\xi'^*\cdot\xi] - G_3(Q^2)\frac{(\xi'^*\cdot q)(\xi\cdot q)}{2m_d^2}\right\}(d^\mu + d'^\mu) + G_M(Q^2)\,[\xi^\mu(\xi'^*\cdot q) - \xi'^{*\mu}(\xi\cdot q)]\,, \qquad (1)$$

where ξ, d (ξ', d') are the polarization and momentum vectors of the incoming (outgoing)

[1] This talk is a shorter version of a review being prepared for *Journal of Physics G* [1].

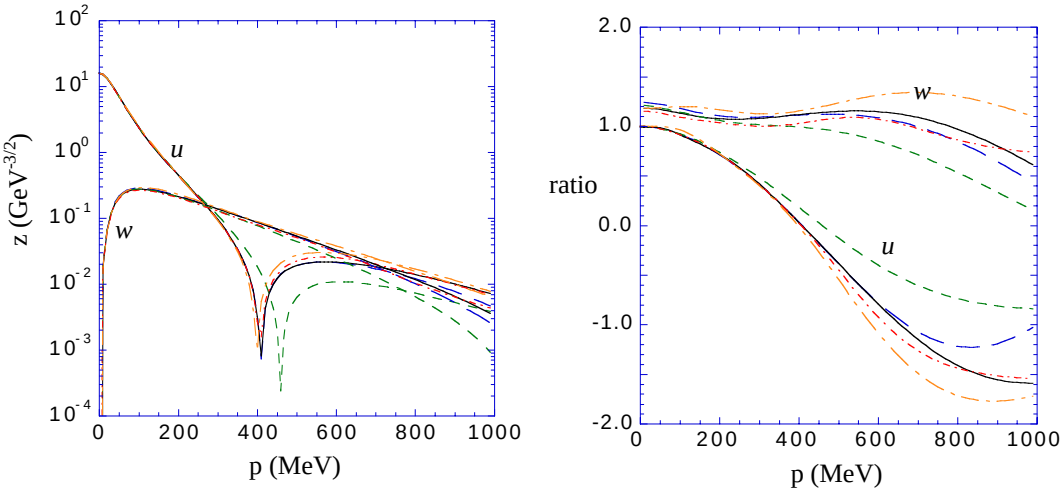

FIGURE 1. Momentum space wave functions for five models mentioned in the text: AV18 (solid), Paris (long dashed), CD Bonn (short dashed), IIB (short dot-dashed), and W16 (long dot-dashed) The wave functions in the right panel have been divided by scaling functions for easy comparison (see Ref. [1] for details).

deuterons, and the form factors $G_i(Q^2)$, $i = 1-3$, are all functions of $Q^2 = -q^2$, the square of the *four*-momentum transferred by the electron, with $q = d' - d$. In practice, G_1 and G_3 are replaced by a more physical choice of form factors

$$\begin{aligned} G_C &= G_1 + \frac{2}{3}\eta\, G_Q \\ G_Q &= G_1 - G_M + (1+\eta) G_3\,, \end{aligned} \tag{2}$$

with $\eta = Q^2/4m_d^2$. At $Q^2 = 0$, the form factors G_C, G_M, and G_Q give the charge, magnetic and quadrupole moments of the deuteron

$$\begin{aligned} G_C(0) &= \quad 1 && (\text{in units of } e) \\ G_Q(0) &= \quad Q_d && (\text{in units of } e/m_d^2) \\ G_M(0) &= \quad \mu_d && (\text{in units of } e/2m_d)\,. \end{aligned} \tag{3}$$

The structure functions A and B, and the polarization transfer coefficient T_{20} depend on the three electromagnetic form factors

$$\begin{aligned} A(Q^2) &= G_C^2(Q^2) + \frac{8}{9}\eta^2 G_Q^2(Q^2) + \frac{2}{3}\eta G_M^2(Q^2) \\ B(Q^2) &= \frac{4}{3}\eta(1+\eta) G_M^2(Q^2) \\ \tilde{T}_{20} &= -\sqrt{2}\,\frac{y(2+y)}{1+2y^2}\,, \end{aligned} \tag{4}$$

where $y = 2\eta G_Q/3G_C$, and $\tilde{T}_{20}$ is T_{20} with the magnetic contributions removed.

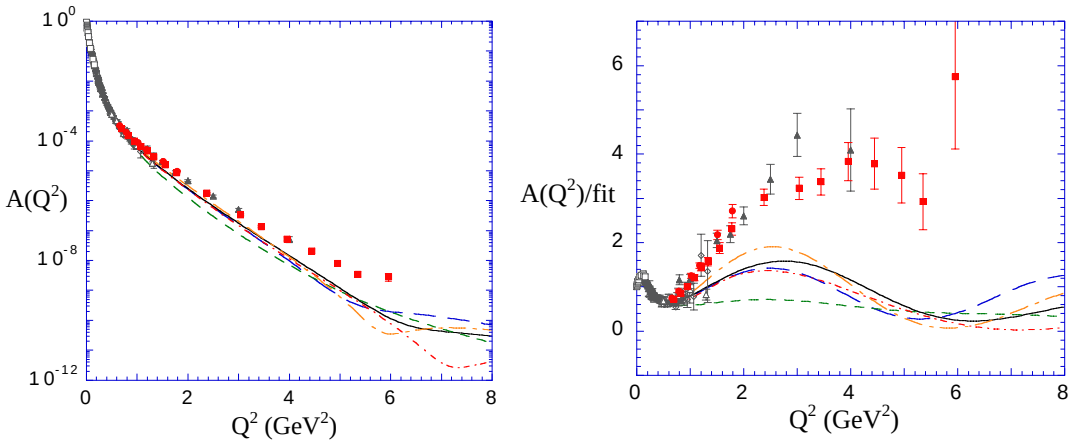

FIGURE 2. The structure function A for five nonrelativistic models using the MMD nucleon form factors. The models are labeled as in Fig. 1. The right panel shows data and models divided by a "fit" described in Ref. [1]. The data are fully referenced in [1].

Comparison of nonrelativistic theory to data

In the nonrelativistic theory, *without exchange currents or* $(v/c)^2$ *corrections*, the deuteron form factors are

$$\begin{aligned} G_C &= G_E^s D_C \\ G_Q &= G_E^s D_Q \\ G_M &= \frac{m_d}{2m_p}\left[G_M^s D_M + G_E^s D_E\right], \end{aligned} \tag{5}$$

where G_E^s and G_M^s are the *nucleon isoscalar* form factors, and the Ds are the *body* form factors. All are functions of Q^2. Hence the study of deuteron form factors is complicated by the fact that they are a *product* of the *nucleon isoscalar* form factors and *body* form factors. The dependence of the deuteron form factors on older models of the nucleon form factors is well discussed in Ref. [13]. A year ago the model of Mergell, Meissner and Drechsel [14] (referred to as MMD) gave a good fit, and could have been adopted as a standard (the new G_{Ep}/G_{Mp} data from JLab [15] may change this view). The high Q^2 data for A provide the most stringent test. In Fig. 2 we compare the data for A with nonrelativistic calculations using the five nonrelativistic wave functions shown in Fig. 1. The calculations use Eq. (5) with MMD isoscalar nucleon form factors and nonrelativistic body form factors. In the right panel the data and models have been divided by the "fit" described in Ref. [1].

It is easy to see that the nonrelativistic models *are a factor 4 to 8 smaller than the data for* $Q^2 > 2$ *GeV*^{2}. Furthermore, since the difference between different deuteron models is substantially smaller than this discrepancy, it is unlikely that any *realistic* nonrelativistic model can be found that will agree with the data. If the nucleon isoscalar charge form factor were larger than the MMD model by a factor of 2 to 3 it might

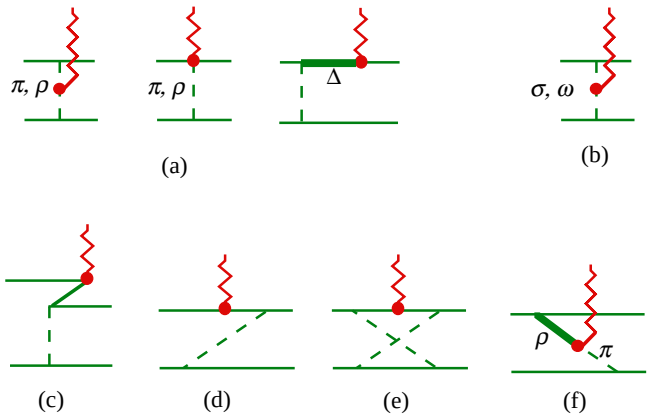

FIGURE 3. Exchange currents that might play a role in meson theories. (a) Large $I = 1$ π,ρ, and Δ currents that do not contribute to the deuteron form factors, and (b) possible $I = 0$ currents that are identically zero. The currents that do contribute to the deuteron form factors are shown in the second row: (c) "pair" currents from nucleon Z-graphs; (d) "recoil" corrections; (e) two pion exchange (TPE) currents; and (f) the famous $\rho\pi\gamma$ exchange current.

explain the data, but this is also unlikely since the variation between nucleon form factor models is substantially smaller than this. We are forced to conclude that these high Q^2 measurements *cannot be explained by nonrelativistic physics and present very strong evidence for the presence of interaction currents, relativistic effects, or possibly new physics.*

Relativistic calculations and new physics

The differences between the data and the nonrelativistic theory can only be explained by a combination of the following effects

- interaction (or meson exchange) currents;
- relativistic effects; or
- new (quark) physics.

The only possibilities excluded from this list are variations in models of the nucleon form factors, or model dependence of the deuteron wave functions. Previously we have argued that *neither* the current uncertainty in our knowledge of the nucleon form factors, *nor* the model dependence of the nonrelativistic deuteron wave functions is sufficient to provide an explanation for the discrepancies.

Possible interaction currents that might account for the discrepancy are shown in Fig. 3. Because the deuteron is an isoscalar system, the familiar large $I = 1$ exchange currents are "filtered" out and only $I = 0$ exchange currents can contribute to the form factors. The $I = 0$ currents tend to be smaller and of a more subtle origin. The nucleon

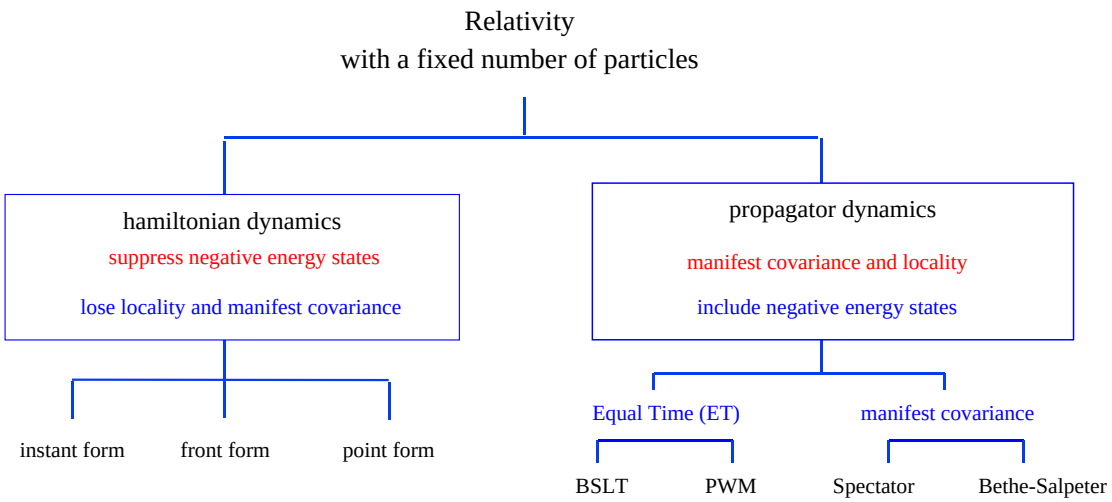

FIGURE 4. The relativistic decision tree discussed in the text.

Z-graphs, Fig. 3c, and the recoil corrections, Fig. 3d, are both of relativistic origin. (The recoil graphs will give a large, incorrect answer unless they are renormalized [16, 17, 18].) The two-meson exchange currents should be omitted unless the force also contains TPE forces. The famous $\rho\pi\gamma$ exchange current is very sensitive to the choice of $\rho\pi\gamma$ form factor, which is hard to estimate and could easily be a placeholder for new physics arising from quark degrees of freedom.

In most calculations based on meson theory, the two pion exchange (TPE) forces and currents are excluded, and, except for the $\rho\pi\gamma$ current (which we will regard as new physics), the exchange currents are of relativistic origin. Additional relativistic effects arise from boosts of the wave functions, the currents, and the potentials, which can be calculated in closed form or expanded in powers of $(v/c)^2$, depended on the method used. At low Q^2 calculations may be done using effective field theories in which a small parameter is identified, and the most general (i.e. exact) theory is expanded in a power series in this small parameter. In these calculations, an expansion of relativistic effects in a power series in $(v/c)^2$ is automatically included. *Hence*, with the exception of effective field theories, *any improvement on nonrelativistic theory using nucleon degrees of freedom leads us to relativistic theory.*

Alternatively, one may seek to explain the discrepancy using quark degrees of freedom (new physics). When two nucleons overlap, their quarks can intermingle, leading to the creation of new *NN* channels with different quantum numbers (states with nucleon isobars, or even, perhaps, so-called "hidden color" states). These models require that assumptions be made about the behavior of QCD in the nonperturbative domain, and are difficult to construct, motivate, and constrain. At very high momentum transfers it may be possible to estimate the interactions using perturbative QCD (pQCD). Very little has been done using other approaches firmly based in QCD, such as lattice gauge theory or Skrymions.

In deciding which relativistic method to use, it is first necessary to decide whether or not to allow *antiparticle, or negative energy* nucleons to propagate as part of the virtual

intermediate state. Since nucleons are heavy and composite, so that their antiparticle states are very far from the region of interest, some physicists believe that intermediate states should be built only from positive energy nucleons, and that all negative energy effects (if any) should be included in the interaction. These methods are referred to collectively as *hamiltonian dynamics* and are represented by the left hand branch shown in Fig. 4. Unfortunately, it turns out that this choice precludes the possibility of retaining the properties of locality and manifest covariance enjoyed by field theory. Alternatively, in order to keep the locality and manifest covariance of the original field theory, other physicists are willing to allow negative energy states into the propagators. These methods, represented by the right-hand branch of the figure, are referred to collectively as *propagator dynamics*. However, including negative energy states tends to make calculations technically more difficult and harder to interpret physically, and those who advocate the use of hamiltonian dynamics do not believe the advantages of exact covariance justify the work it requires.

Unfortunately, these two methods are so fundamentally different that many physicists do not realize that the limitations of one may not apply to the other. For example, for some choices of propagator dynamics all 10 of the generators of the Poincaré group will depend only on the kinematics, and the Poincaré transformations of *all amplitudes can be done exactly*. With hamiltonian dynamics this is not the case; some of the 10 generators must depend on the interaction, and transformation of matrix elements under these "dynamical" transformations must be calculated. Comparison of the two methods is therefore very difficult; the language and issues of each are very different and one can be easily misled by the different appearance of the results.

Comparison of relativistic calculations with data

The high Q^2 predictions for 7 relativistic models using *NN* degrees of freedom and one quark cluster model are shown in Figs. 5–6. They include

- two propagator calculations: VGO [19] (using the Spectator equation), and PWM [20] (using the modified Mandelzweig-Wallace equation);
- two instant-form calculations: FSR [21] (without a v/c expansion) and ARW [22] (using a v/c expansion);
- two front-form calculations: CK [23] (with the light front retained as an unphysical degree of freedom) and LPS [24] (using a specially constructed current operator);
- a point-form calcualtion: AKP [25]; and
- a quark model calculation: DB [26].

The model dependence of the eight calculations is large. Figure 5 shows the predictions for $A(Q^2)$. In these figures we have intentionally left out the model dependent $\rho\pi\gamma$ exchange current from all of the calculations. All of the models except the AKP point-form calculation give a reasonable description of A out to $Q^2 \sim 3$ GeV^2, beyond which they begin to depart strongly from each other and the data. Taking into account that the $\rho\pi\gamma$ exchange current *could be added to any of these models, and that this contribution tends to increase A above* $Q^2 \sim 3$ *GeV*^{2}, four models seem to have the right general

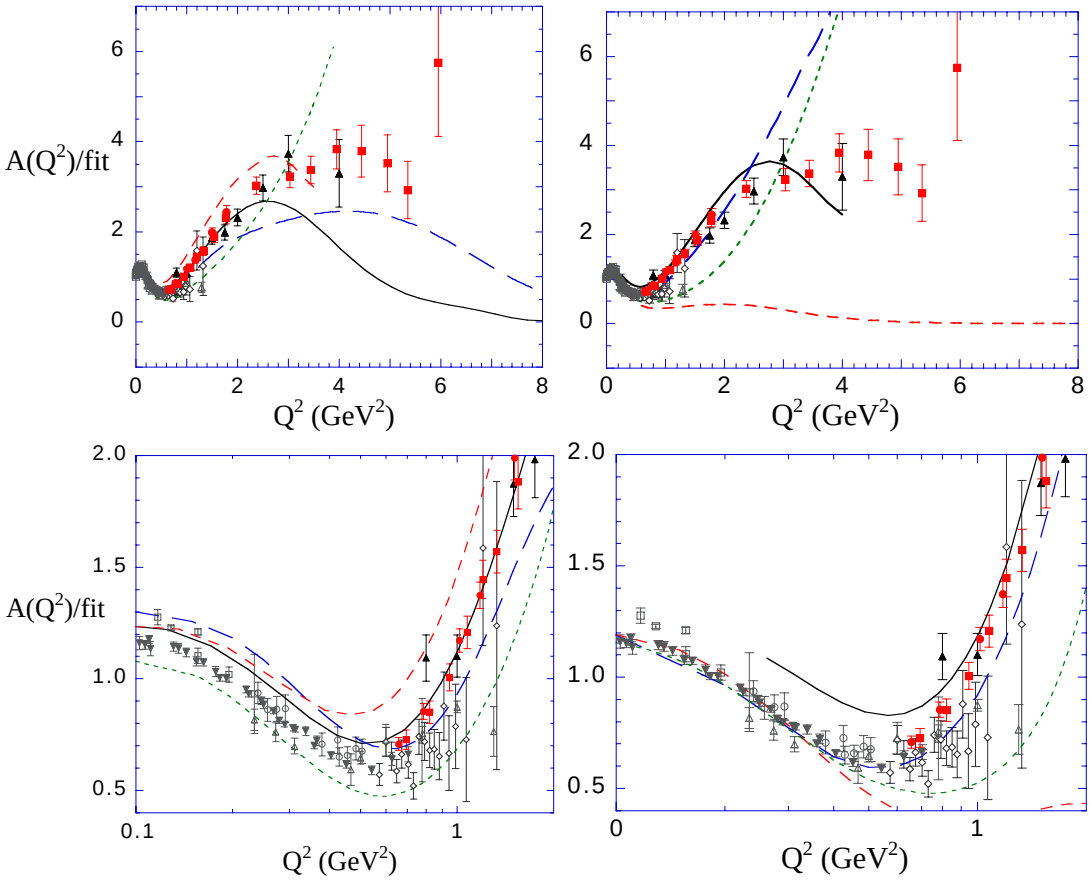

FIGURE 5. The structure function A for the eight models discussed in the text. Left panels show the propagator and instant-form results: FSR (solid line), VOG in RIA approximation (long dashed line), ARW (short dashed line), and PWM (dotted line). Right panels show the front-form CK (long dashed line) and LPS (short dashed line), the point-form AKP (medium dashed line) and the quark model calculation DB (solid line). In every case the calculations have been divided by a scaling function given in Ref. [1]. The data are labeled as in Fig 2.

behavior: the VOG, FSR, ARW and the quark model of DB (but there are no results for this model beyond $Q^2 = 4$ GeV^2). None of these models fit the data without a $\rho\pi\gamma$ exchange current, and all models would be improved by adding such a current contribution, *showing that there is some evidence for new physics at high* Q^2. Ironically, none of the models favored by the high Q^2 data does as well at low Q^2 as the three "unfavored" models shown in the right panels (unless the Platchkov [27] data are systematically too low).

Finally, Fig. 6 shows the predictions for the structure functions A, B, and T_{20} for the eight models. The LPS calculation shows a large discrepancy with the T_{20} data, but the most striking feature of these plots is the *large model dependence* of the predictions for $B(Q^2)$. The magnetic structure function provides the most stringent test of the models,

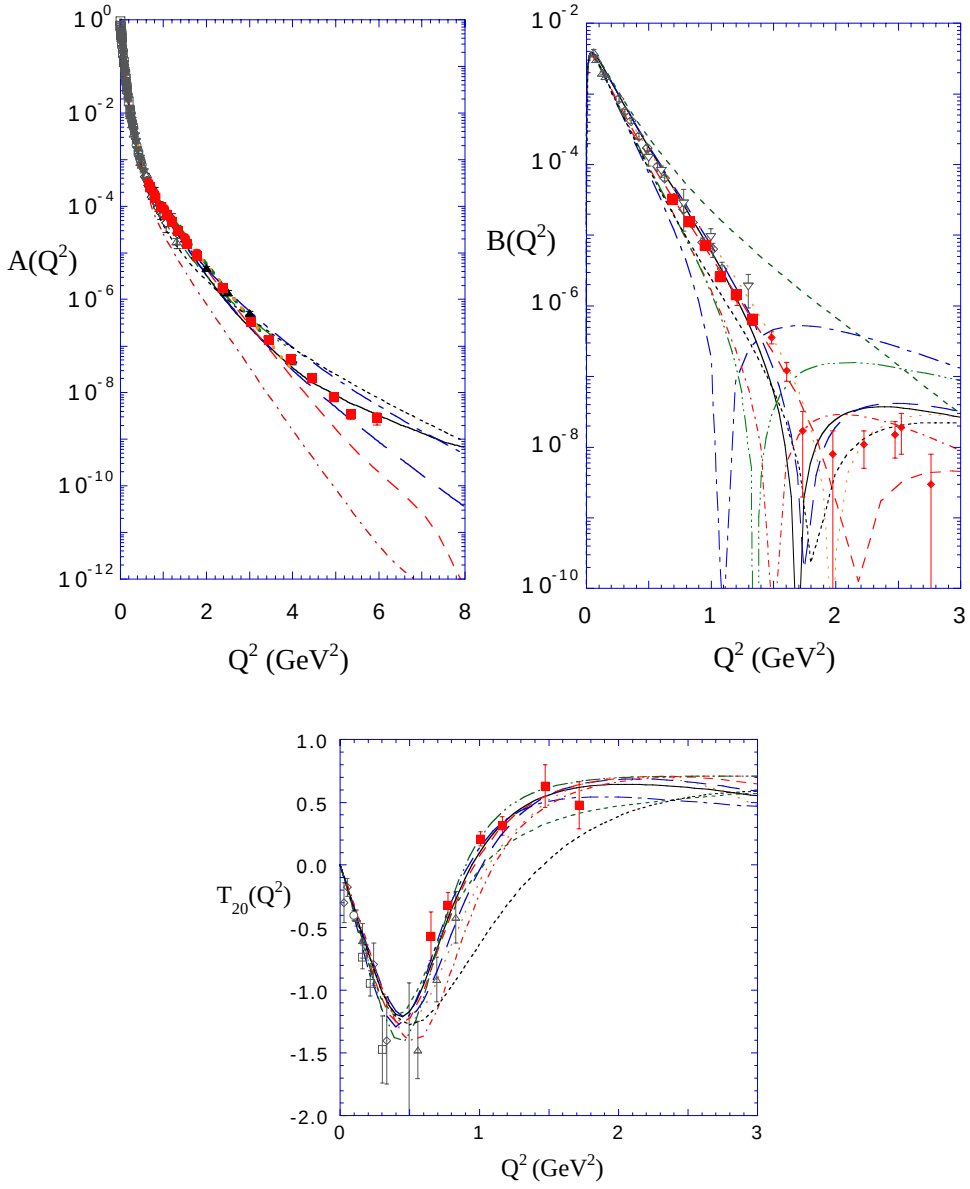

FIGURE 6. The structure functions *A*, *B*, and T_{20} for the eight models discussed in the text. VOG full calculation (CIA plus $\rho\pi\gamma$ – solid line); VOG in RIA (long dashed line); FSR (medium dashed line); ARW (short dashed line); DB (widely spaced dotted line); CK (long dot-dashed line); AKP (short dot-dashed line); PWM (dashed double-dotted line), and LPS (dotted line). The data are as labeled in Fig. 2.

and the predictions are comparatively free of the $\rho\pi\gamma$ exchange current (which gives only a small contribution to *B*). Examination of the figure shows that the *B* predictions of the PWM, ARW, AKP, CK models fare the worst. In all, taking the predictions for the three structure functions together, the best results are obtained with the FSR, VOG, and DB models.

Conclusions (deuteron form factors)

What have we learned from our measurements of the deuteron form factors? Our comparison of theory and experiment leads to the following conclusions:

- Nonrelativistic quantum mechanics (without exchange currents or relativistic effects) is ruled out by the $A(Q^2)$ data at high Q^2. Reasonable variations in nucleon form factors or uncertainties in the nonrelativistic wave functions cannot remove the discrepancies.
- In approaches using NN degrees of freedom only, relativistic effects (or $I = 0$ meson exchange currents) could be large enough to explain the data.
- Some models that include relativistic effects (or meson exchange currents) and use NN degrees of freedom with realistic forces are close to the data. None are entirely satisfactory.
- The model dependence of relativistic effects (or meson exchange currents) is larger than the errors in the data, even at low Q^2, and is not understood.
- There is evidence that new physics (either in the from of the $\rho\pi\gamma$ exchange current or something else) is beginning to show up in the A structure function above Q^2 of 2 - 3 GeV^2.
- The deuteron form factors provide no evidence for the onset of pQCD, but quark cluster models could explain the data.

Study of the experimental situation leads to the following conclusions:

- The minimum of B is very sensitive to details of the models, and improved measurements of B for Q^2 in the region 1.5 - 4 GeV^2 are particularly compelling. It is important to accurately map out the zero in the B structure function.
- Detailed disagreements between theories and different data sets suggests the need for precision studies at low Q^2.

THRESHOLD ELECTRODISINTEGRATION

Threshold deuteron electrodisintegration measures the $d(e,e')pn$ reaction in kinematics in which the proton and neutron, rather than remaining bound, are unbound with a few MeV of relative kinetic energy in their center of mass system. If the final state energy is low enough, the final state will be dominated by transitions to the $^1S_0$ final state, and will be a pure $\Delta S = 1$, $\Delta I = 1$, $M1$ transition, similar to the $N \rightarrow \Delta(1232)$ transition. This transition is a companion to the B structure function; both are magnetic transitions and both are filters for exchange currents with only one isospin ($d \rightarrow d$ is $\Delta I = 0$ and $d \rightarrow {}^1S_0$ is $\Delta I = 1$). To see the similarity, compare the top right panel of Fig. 6 with the threshold measurements shown in left panel of Fig. 7. Both have a similar shape, and in both cases the uncertainties in the theoretical predictions are large.

The similarity of these two processes (elastic and threshold inelastic) also holds for the theory. These two processes can be used to separately determine the precise details of the $I = 0$ and $I = 1$ exchange currents. Once the exchange currents are fixed, they can

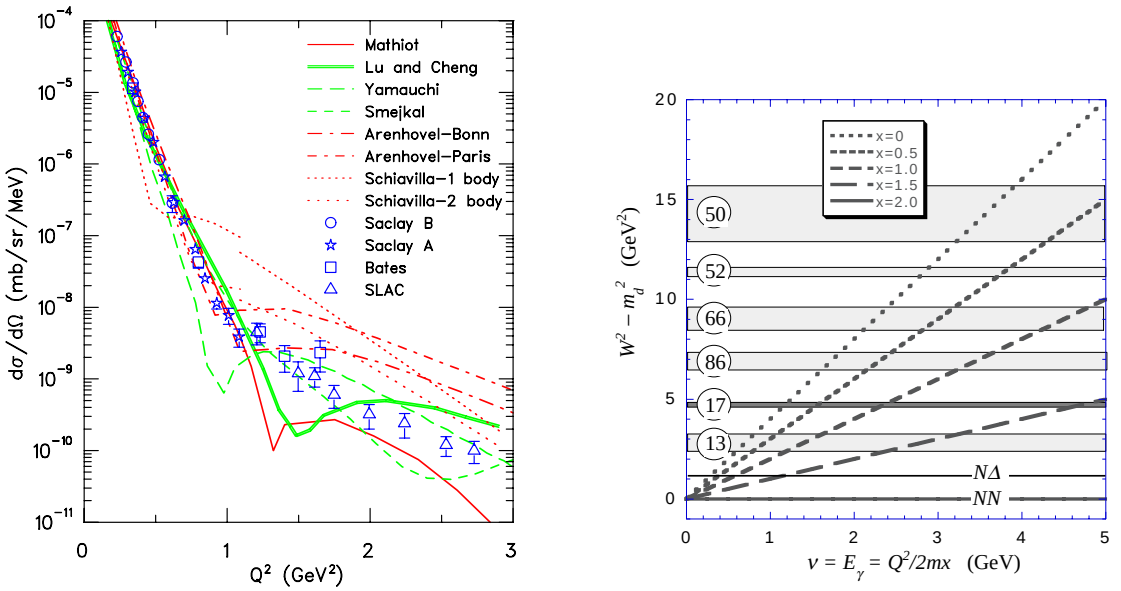

FIGURE 7. Left panel: The cross section for threshold electrodisintegration of the deuteron. (See Ref. [1] for discussion of the data and the theory.) Right panel: The variation of W^2 with the photon energy ν for various values of x. The shaded regions show the approximate thresholds for the production of bands of nucleon resonances. The numbers in the small circles are the number of distinct channels in each band.

be used to predict the results of $d(e,e'p)n$ over a wide kinematic region. Any theoretical approach that works for the form factors should also work equally well for threshold electrodisintegration, yet very few of the groups who have calculated form factors have also calculated the threshold process. These calculations, when completed, will provide a more definitive test of the various relativistic approaches discussed in the previous sections.

DEUTERON PHOTODISINTEGRATION

Since *both* the recent deuteron form factor measurements *and* the recent high energy deuteron photodisintegration measurements have been made with 4 GeV electron beams, it is sometimes assumed that the same theory should work for both. This need not be the case, because the kinematics of elastic electron-deuteron scattering and deuteron photodisintegration are very different, and the physics being explored by these two measurements is also very different. The implications of this remarkable feature of electronuclear physics is often not fully appreciated.

The kinematics of elastic scattering and photodisintegration are compared in the right panel of Fig. 7, which shows $W^2 - m_d^2$ as a function of the photon (real or virtual) energy. Here $x = Q^2/(2m\nu)$ is the familiar Bjorken scaling variable. The mass of the final excited state increases rapidly as x decreases below its maximum allowed value of $x = m_d/m \simeq 2$. For any energy ν or any Q^2, elastic *ed* scattering leaves the *pn*

system bound, with no internal excitation energy added to the two nucleons. As $x \rightarrow 0$ (the real photon limit) the maximum value of W is reached for any given beam energy. The 24 well established nucleon resonances, and the bands of thresholds at which these resonances are excited, are show in Fig. 7. At E_γ = 4 GeV, the final state mass is approximately 4.5 GeV, and at least 286 thresholds for the production of pairs of baryon resonances have been crossed (and there are probably more from unseen or weakly established resonances). A photon energy of 4 GeV corresponds to np scattering with an np laboratory kinetic energy of about 8 GeV!

It is clearly very difficult (if not impossible) to construct a theory of high energy photoproduction in which all of these resonances and their corresponding 286 production thresholds are treated microscopically. By contrast, elastic electron deuteron scattering requires a microscopic treatment of only *one channel*. All of the 286 channels also contribute to elastic scattering, of course, but in this case they are *not explicitly excited*, and can probably be well described by slowly varying short-range terms included in a meson exchange (or potential) model. In photodisintegration, *each of these channels is excited explicitly* and an alternate framework that *averages over the effects of many hadronic states* is needed. The alternatives are to use a Glauber-like approach, or to borrow from our knowledge of DIS and build models that rely on the underlying quark degrees of freedom.

High Energy Photodisintegration

Figure 8 shows the published high energy photodisintegration data, from experiments NE8 [28, 29] and NE17 [30] at SLAC, and E89-012 [31] and E96-003 [32] at CEBAF. These experiments determine cross sections for $\theta_{cm} \approx 36^\circ$, 52°, 69°,and 89° at energies from about 0.7 to 5.5 GeV; there are also some backward angle data up to 1.6 GeV from NE8.

The main feature of the data above about 1 GeV is the s^{-11} (s^{-10}) fall off (where $s = (p_1 + p_2)^2$ is the square of the cm. energy) of the cross sections $d\sigma/dt$ ($d\sigma/d\Omega$) at θ_{cm} = 90 and 69°, in agreement with perturbative QCD expectations. In contrast, the cross sections at the forward angles 36 and 52°, fall off more slowly, with $\approx s^{-9}$ scaling at lower energies, until the onset of the s^{-11} behavior at about 4 and 3 GeV beam energy, respectively. At each angle the onset of the s^{-11} behavior corresponds to a perpendicular momentum, p_T, of approximately 1 GeV^2.

The highest energy polarization measurements are of p_y (the induced polarization of the proton), and $C_{x'}$ and $C_{z'}$ (the transfer of circular polarization from the photon to the proton) from CEBAF E89-019 [33]. The left panel of Fig. 9 shows the striking feature that the induced polarization p_y is consistent with zero (as predicted by pQCD) at energies above about 1 GeV, the same energy at which the s^{-11} cross section scaling begins. The right panel of the same figure shows that the polarization transfer observables both appear to peak near 1 GeV, and decrease at higher energies.

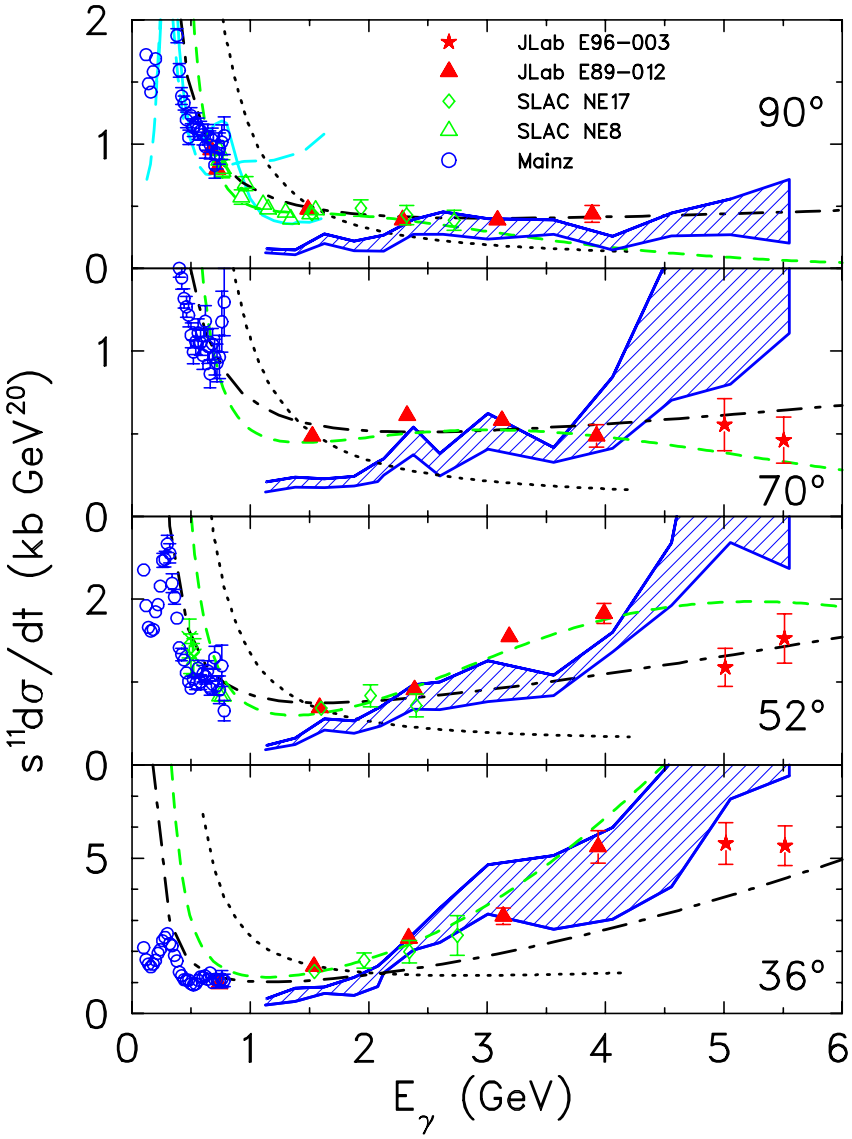

FIGURE 8. Photodisintegration cross section $s^{11}d\sigma/dt$ versus incident lab photon energy. The calculations are from Kang, Erbs, Pfeil and Rollnik (solid line), Lee (dashed line), Raydushkin quark exchange (dot-dashed line), reduced nuclear amplitudes of Brodsky Hiller (dotted line), quark qluon string model (short dashed line), and Frankfurt, Miller, Strikman and Sargsian QCD rescattering (shaded region). (See Ref. [1] for references and discussion of the data and theory.)

Conclusions (deuteron photodisintegration)

Review of deuteron photodisintegration suggests the following:

- A microscopic meson-baryon theory of deuteron photodisintegration must describe the NN interaction at high energies, including pion production and the contributions of hundreds of N^* channels. It is unlikely that such a theory will be constructed in the foreseeable future.

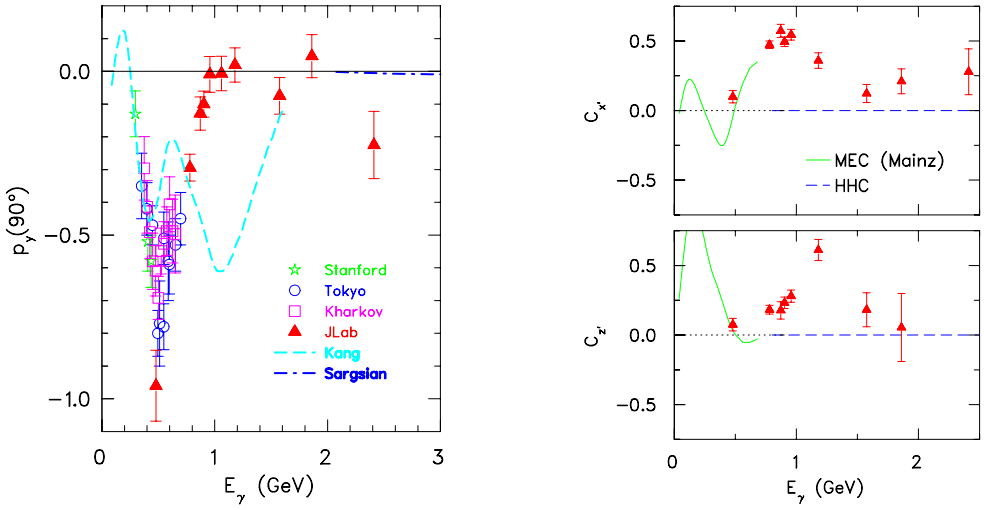

FIGURE 9. Left panel: Induced polarization for deuteron photodisintegration at $\theta_{cm} = 90°$. The calculations are from Kang, Erbs, Pfeil and Rollnik (dashed line) and from Sargsian (dot-dashed line). Right panel: Polarization transfer for deuteron photodisintegration at $\theta_{cm} = 90°$. The calculation is from Schwamb and Arenhövel.

- For $p_T^2 > 1$ GeV^2, cross sections appear to follow the constituent counting rules, but it is expected that an absolute pQCD calculation would greatly underpredict the data. Similar observations may be made for other photoreactions, and it remains to be seen how this behavior arises, and if there is a general explanation for it.
- Some nonperturbative quark models do well describing the data qualitatively. Further theoretical development and experimental tests of these models would be desirable.

OVERALL CONCLUSIONS

Our overall conclusions from the study of form factors and high energy photodisintegration can be briefly summarized as follows:

- Meson theory works well in cases where all of the *active* hadronic channels that can contribute to a process are included. This has been done for the deuteron form factors (where only the NN channel is active), but is impossible for high energy deuteron photodisintegration where 100's of N^*N^* channels are active. At high energy, any successful meson theory must include relativistic effects.
- New approaches, probably using quark degrees of freedom, are needed for high energy deuteron photodisintegration.
- Meson theory behaves as might be expected. It works for the deuteron form factors and does not work for photodisintegration (because of the number of channels).
- Perturbative QCD does not behave as might be expected. Theoretically it should work (or not work) equally well for the deuteron form factors at high Q^2 as it does for photodisintegration at high $p_\perp^2$ (both are exclusive processes). However

the scaling laws seem to work qualitatively for photodisintegration and to fail badly for elastic scattering.

Please refer to Ref. [1] for a more complete discussion of all of the points in this talk.

ACKNOWLEDGMENTS

This work was supported in part by the US Department of Energy. The Southeastern Universities Research Association (SURA) operates the Thomas Jefferson National Accelerator Facility under DOE contract DE-AC05-84ER40150.

REFERENCES

1. Gilman, R., and Gross, F., to be submitted to *Journal of Physics G*.
2. Lancombe, M., Loiseau, B., Richard, J.M., Vinh Mau, R., Côté, J., Pirès, P., and de Tourreil, R., *Phys. Rev.* C **21**, 861 (1980).
3. Wiringa, R.B., Stoks, V.G.J., and Schiavilla, R., *Phys. Rev.* C **51**, 38 (1995).
4. Stoks, V.G.J., Klomp, R.A.M., Terheggen, C.P.F., and de Swart, J.J., *Phys. Rev.* C **49**, 2950 (1994).
5. Machleidt, R., Sammarruca, F., and Song, Y., *Phys. Rev.* C **53**, R1483 (1996).
6. Machleidt, R., *Phys. Rev.* C **63**, 024001 (2001).
7. Gross, F., Van Orden, J.W., and Holinde, K., *Phys. Rev.* C **45**, 2094 (1992).
8. Stadler, A., and Gross, F., *Phys. Rev. Lett.* **78**, 26 (1997).
9. Gross, F., *Phys. Rev.* **136**, B140 (1965).
10. Arnold, R.E., Carlson, C.E., and Gross, F., *Phys. Rev.* C **21**, 1426 (1980).
11. Donnelly, T.W., and Raskin, A.S., *Ann. Phys. (N.Y.)* **169**, 247 (1986).
12. Jones, H., *Nuovo Cimento* **26**, 790 (1962).
13. Garçon, M., and Van Orden, J.W., preprint nucl-th/0102049, *Advances in Nucl. Phys.* **26**, (2001).
14. Mergell, P., Meissner, Ulf-G., and Drechsel, D., *Nucl. Phys.* A **596**, 367 (1996).
15. Jones, M., *et al.*, *Phys. Rev. Lett.* **84**, 1398 (2000).
16. Gross, F., published in *Modern Topics in Electron Scattering* (ed. Frois, B., and Sick, I., 1991), p. 219
17. Jackson, A.J., Lande, A., and Riska, D.O., *Phys. Lett.* B **55**, 23 (1975).
18. Thompson, R.H., and Heller, H., *Phys. Rev.* C **7**, 2355 (1973).
19. Van Orden, J.W., Devine, N., and Gross, F., *Phys. Rev. Lett.* **75**, 4369 (1995).
20. Phillips, D.R., Wallace, S.J., and Devine, N.K., *Phys. Rev.* C **58**, 2261 (1998).
21. Forest, J., and Schiavilla, R., (private communication – to be published)
22. Arenhövel, H., Ritz, F., and Wilbois, T., *Phys. Rev.* C **61**, 034002 (2000).
23. Carbonell, J., and Karmanov, V.A., *Eur. Phys. J* A **6**, 9 (1999).
24. Lev, F.M., Pace, E., and Salmé, G., *Phys. Rev.* C **62**, 064004 (2000).
25. Allen, T.W., Klink, W.H., and Polyzou, W.N., *Phys. Rev.* C **63**, 034002 (2001).
26. Dijk, H., and Bakker, B.L.G., *Nucl. Phys.* A **494**, 438 (1988).
27. Platchkov, S., *et al.*, *Nucl. Phys.* A **510**, 740 (1990).
28. Napolitano, J., *et al.*, *Phys. Rev. Lett.* **61**, 2530 (1988).
29. Freedman, S.J., *et al.*, *Phys. Rev.* C **48**, 1864 (1993).
30. Belz, J.E., *et al.*, *Phys. Rev. Lett.* **74**, 646 (1995).
31. Bochna, C., *et al.*, *Phys. Rev. Lett.* **81**, 4576 (1998).
32. Schulte, E., *et al.*, *Phys. Rev. Lett.* **87**, 102302 (2001).
33. Wijesooriya, K., *et al.*, *Phys. Rev. Lett.* **86**, 2975 (2001).